




6-2013

Projected Surface Finite Elements for Elliptic Equations

Necibe Tuncer
University of Tulsa

Follow this and additional works at: <https://digitalcommons.pvamu.edu/aam>

 Part of the [Algebraic Geometry Commons](#), [Numerical Analysis and Computation Commons](#), and the [Partial Differential Equations Commons](#)

Recommended Citation

Tuncer, Necibe (2013). Projected Surface Finite Elements for Elliptic Equations, Applications and Applied Mathematics: An International Journal (AAM), Vol. 8, Iss. 1, Article 2.
Available at: <https://digitalcommons.pvamu.edu/aam/vol8/iss1/2>

This Article is brought to you for free and open access by Digital Commons @PVAMU. It has been accepted for inclusion in Applications and Applied Mathematics: An International Journal (AAM) by an authorized editor of Digital Commons @PVAMU. For more information, please contact hvkoshy@pvamu.edu.



Projected Surface Finite Elements for Elliptic Equations

Necibe Tuncer

Department of Mathematics
University of Tulsa
800 S. Tucker Drive, Tulsa, OK, 74104
necibe-tuncer@utulsa.edu

Received: Received: September 13, 2012; Accepted: May 16, 2013

Abstract

In this article, we define a new finite element method for numerically approximating solutions of elliptic partial differential equations defined on “arbitrary” smooth surfaces S in \mathbb{R}^{N+1} . By “arbitrary” smooth surfaces, we mean surfaces that can be implicitly represented as level sets of smooth functions. The key idea is to first approximate the surface S by a polyhedral surface S_h , which is a union of planar triangles whose vertices lie on S ; then to project S_h onto S . With this method, we can also approximate the eigenvalues and eigenfunctions of the Laplace-Beltrami operator on these “arbitrary” surfaces.

Keywords: Laplace-Beltrami operator; finite element method on surfaces; eigenvalue problem

MSC 2010 No.: 65N30; 65N50; 65N25; 35P15; 58J99

1. Introduction

Numerical methods to solve partial differential equations defined on surfaces have been studied by many authors (Apel and Pester, 2005; Demlow and Dziuk, 2007; Dziuk, 1988; Dziuk and Elliott, 2007; Holst, 2001; Meir and Tuncer, 2009). In order to focus on the basic issues arising in analysis of the numerical methods used to approximate the solutions of such partial differential

equations, we consider the following classical elliptic partial differential equation

$$-\Delta_S u + u = f. \quad (1)$$

Here Δ_S is the Laplace-Beltrami operator, and $S \in \mathbb{R}^{N+1}$ is a smooth, compact surface with no boundary. The Laplace-Beltrami operator on the surface S is defined to be the tangential divergence of the tangential gradient:

$$\Delta_S u = \nabla_S \cdot \nabla_S u,$$

where the tangential gradient and divergence are defined as follows,

$$\nabla_S u = \nabla u - (\nabla u \cdot n)n,$$

$$\nabla_S \cdot u = \nabla \cdot u - \sum_{i=1}^{N+1} ((\nabla u_i) \cdot n)n_i.$$

The existence and uniqueness of (1) is classical; there exists a unique solution u to (1) (Aubin, 1980). The weak formulation of (1) is: Find $u \in H^1(S)$ s.t.

$$\int_S \nabla_S u \cdot \nabla_S v + \int_S uv = \int_S fv \quad \forall v \in H^1(S). \quad (2)$$

Galerkin method for approximating (2) is simply defining a similar problem within a finite dimensional subspace χ_h of $H^1(S)$. So, the discrete weak formulation of (2) is:

Find $u^h \in \chi_h$ s.t.

$$\int_S \nabla_S u^h \cdot \nabla_S v^h + \int_S u^h v^h = \int_S f v^h \quad \forall v^h \in \chi_h. \quad (3)$$

Mesh generation is an important part of the whole approximation process of the the partial differential equations, since the accuracy of numerical solutions depend on the quality of the mesh. There are several approaches to generate meshes on surfaces, some of these approaches have been studied in (Apel and Pester, 2005; Du and Ju, 2005; Dziuk, 1988; Holst, 2001). The two main approaches are *i*) to generate the mesh on a linear approximation of the surface, see (Dziuk, 1988), *ii*) to generate the mesh directly on the surface, see (Du and Ju, 2005). In this paper we will follow the second approach and thus, construct the mesh directly on the surface. The first approach is discussed in detail in (Dziuk, 1988). The main idea for the finite element method for the Laplace-Beltrami equation on arbitrary surfaces introduced in (Dziuk, 1988) is to approximate the surface S with a polyhedral (polygon if $N = 1$) surface S_h . Following the method introduced in (Dziuk, 1988), the discrete weak formulation of (2) is as follows: Find $u^h \in X_h$ s.t.

$$\int_{S_h} \nabla_{S_h} u^h \cdot \nabla_{S_h} v^h + \int_{S_h} u^h v^h = \int_{S_h} f^h v^h \quad \forall v^h \in X_h, \quad (4)$$

where X_h is the finite dimensional subspace of $H^1(S_h)$ and f^h is projection of f onto S_h . Clearly $X_h \subset H^1(S_h)$, but not a subset of $H^1(S)$. The error estimate in the theory of finite element method is based on Cea's Lemma which uses the fact that (Brenner and Scott, 1994)

$$\chi_h \subset H^1(S). \quad (5)$$

Clearly, the family of finite element spaces X_h constructed in (4) violates (5). This violation is almost inevitable in finite element methods on surfaces, since the surface, S , is approximated by S_h . In this paper we develop a finite element method for arbitrary surfaces such that (5) is not violated, thus we develop a conforming finite element method.

We define a new method which would yield a family of finite element spaces χ_h , s.t. $\chi_h \subset H^1(S)$. With our method we approximate the solutions of elliptic partial differential equations on the surface S , not on its any approximation. In the theory of finite element method there are two sources of error in the error analysis; the first source comes from replacing the infinite dimensional space with a finite dimensional one, and the second source comes from approximating the domain S by S_h . We propose a new method that would eliminate the error source caused by approximating the surface S . With our method, the discrete weak formulation of (2) is as follows: Find $u^h \in \chi_h$ s.t.

$$\int_S \nabla_S u^h \cdot \nabla_S v^h + \int_S u^h v^h = \int_S f v^h \quad \forall v^h \in \chi_h. \quad (6)$$

The main idea behind our new method is as follows: Let S_h be a an approximation of S which consists of planar triangles T_h whose vertices lie on S . We construct a finite element space on S , by first constructing it on S_h , and then projecting onto S . A finite element space is defined by taking the set of all continuous functions on S , which are linear affine on each planar triangle T_h . Thus, we use S_h as a tool in our computations. This method is proposed in (Demlow, 2009). This method highly depends on the transformation projecting S_h onto S , and inverse transformation projecting S onto S_h . These transformations are crucial in analyzing and implementing the method. In this paper, we focus on this important detail by demonstrating the transformations and their jacobians in numerical experiments. In addition to analyzing the method, we also give explicitly what these transformations are for arbitrary surfaces. Furthermore we add how to use this method to approximate the eigenvalues of arbitrary surfaces. Our method requires a very little computational effort since all computations are done in logically planar domains which easily allows for adaptive mesh refinement and multigrid methods.

1.1. Preliminaries and basic notation

We assume that S is a compact, smooth, connected and oriented n -dimensional surface embedded in \mathbb{R}^{N+1} . For simplicity, we assume that S has a representation defined by a distance function $d(x)$, $x \in \mathbb{R}^{N+1}$ so that,

$$S = \{x \in U, d(x) = 0\},$$

where U is an open subset of \mathbb{R}^{N+1} containing S , in which $\nabla d \neq 0$. Thus, we define $U \subset \mathbb{R}^{N+1}$ to be an open neighborhood such that for every $x \in U$ $d(x) = \text{dist}(x, S) < \delta$, where δ is bounded

by the principle curvatures of S (Gilbarg and Trudinger, 1977). That is, let $\{\kappa_i\}_{i=1}^N$ denote the principal curvatures of S , then (Gilbarg and Trudinger, 1977)

$$\delta < \frac{1}{\max_{i=1,\dots,N} \kappa_i}. \quad (7)$$

Distance function $d(x)$ is a signed distance function in the sense that $d < 0$ inside S and $d > 0$ outside S . The normal to S in the direction of increasing d is given by

$$n = \frac{\nabla d}{|\nabla d|}.$$

Without loss of generality throughout this paper, we assume that $|\nabla d| = 1$. Note that the distance function $d(x)$ is Lipschitz continuous (Gilbarg and Trudinger, 1977). This can be easily shown: Let $x, y \in \mathbb{R}^{N+1}$, and let $b \in S$, such that $d(y) = \|y - b\|$, then $d(x) \leq \|x - b\| \leq \|x - y\| + \|y - b\|$. Thus, $|d(x) - d(y)| \leq \|x - y\|$.

We then define the following projection onto S , for each $x \in U$,

$$P(x) = x - d(x)n,$$

where $P(x) \in S$ and n is the unit normal to S at the point $P(x)$. For any function u which is differentiable in U , we define the tangential gradient on S by,

$$\nabla_S u = \nabla u - (\nabla u \cdot n)n,$$

where for any $x, y \in \mathbb{R}^{N+1}$, $x \cdot y$ denotes the regular inner product and ∇ denotes the regular gradient. We denote the components of the regular gradient as $\nabla = (D_1, \dots, D_{N+1},)$ and the components of tangential derivative as $\nabla_S = (D_{S_1}, \dots, D_{S_{N+1}})$. Note that unlike the regular gradient, the higher order tangential derivatives do not commute. The tangential gradient is the projection of the regular gradient onto the tangent plane, thus $\nabla_S u \cdot n = 0$.

2. Finite Element Approximation

We are interested in the following elliptic partial differential equation

$$-\Delta_S u + u = f \quad \text{on } S. \quad (8)$$

We adopt the standard notation for Lebesgue and Sobolev spaces defined on manifolds, see (Hebey, 1991).

$$L^p(S) = \left\{ u : \int_S \|u\|^p < \infty \right\}; \quad (9)$$

and define

$$H^1(S) = \{u \in L^2(S) : \nabla_S u \in L^2(S)^{N+1}\}.$$

If $\partial S \neq \emptyset$, then $H_0^1(S)$ is also defined in the obvious way, thus it is the closure of $C_0^1(S)$ with respect to the $H^1(S)$ -norm. Similarly, assuming S is smooth enough, we define the Sobolev Spaces $H^m(S)$ for $m \in \mathbb{N}$.

Given $f \in L^2(S)$, there exists a (unique) solution $u \in H^2(S)$ to (8) furthermore there exists a constant c such that

$$\|u\|_{H^2(S)} \leq c\|f\|_{L^2(S)},$$

see, e.g., (Aubin, 1980).

A weak formulation of (8) is, given $f \in H^1(S)^*$ (the dual of $H^1(S)$) find a function $u \in H^1(S)$ such that

$$\int_S \nabla_S u \cdot \nabla_S v + uv = \int_S f v \quad \forall v \in H^1(S), \quad (10)$$

where the right hand side is understood as duality pairing. Let $a(\cdot, \cdot) : H^1(S) \times H^1(S) \rightarrow \mathbb{R}$ be the bilinear form defined by

$$a(u, v) := \int_S \nabla_S u \cdot \nabla_S v + uv. \quad (11)$$

Obviously the bilinear form $a(\cdot, \cdot)$ is continuous and elliptic, since $\|u\|_{H^1(S)} = \sqrt{a(u, u)}$. Given a linear functional $f : H^1(S) \rightarrow \mathbb{R}$

$$(f, v) := \int_S f v,$$

by the Lax-Milgram Lemma there exists a unique solution to (10), see, e.g., (Brenner and Scott, 1994).

Let χ_h be a finite dimensional subspace of $H^1(S)$, then a discrete weak formulation of (10) is, given $f \in L^2(S)$ find $\tilde{u} \in \chi_h$ such that

$$a(\tilde{u}, \tilde{v}) = (f, \tilde{v}) \quad \forall \tilde{v} \in \chi_h. \quad (12)$$

Let $\{\varphi_i\}_{i=1}^n$ be a basis for χ_h , then any $\tilde{u} \in \chi_h$ can be written as $\tilde{u} = \sum_{i=1}^n \tilde{u}_i \varphi_i$. Substituting \tilde{u} in (12) by and setting $\tilde{v} = \varphi_i$, $i = 1, \dots, n$ leads to a linear system of algebraic equation $M\mathbf{x} = \mathbf{f}$ that is uniquely solvable. Here M is the sparse, symmetric, positive definite matrix with entries $(M)_{ij} = a(\varphi_j, \varphi_i)$ and the vectors $\mathbf{f}_i = (f, \varphi_i)$ and $\mathbf{x}_i = \tilde{u}_i$.

Let S_h be a polyhedral approximation of the the surface S , that is S_h consists of union of planar triangles, T_h , such that the nodes of such triangles are on the surface S . Let X_h denote the finite element space on the polyhedral surface S_h , that consists of piecewise linear functions, i.e.,

$$X_h = \{u_h : u_h \text{ is a piecewise linear continuous polynomial on } S_h\}.$$

Let $\{\eta_i\}_{i=1}^n$ be the nodes of the triangulation, and let $\{\varphi_{h_i}\}_{i=1}^n$ be a basis for X_h , such that $\varphi_{h_i}(\eta_j) = \delta_{ij}$, where δ_{ij} is the Kronecker-delta. Setting $\varphi_i = \varphi_{h_i} \circ P^{-1}$, $i = 1, \dots, n$ we get a basis $\{\varphi_i\}_{i=1}^n$ for χ_h . We call $\{\varphi_i\}_{i=1}^n$ as projected surface finite element basis functions. We then define the finite dimensional space χ_h as:

$$\chi_h = \{\tilde{u} : \tilde{u} = u_h \circ P^{-1}, u_h \text{ is a piecewise linear, continuous polynomial on } S_h\}. \quad (13)$$

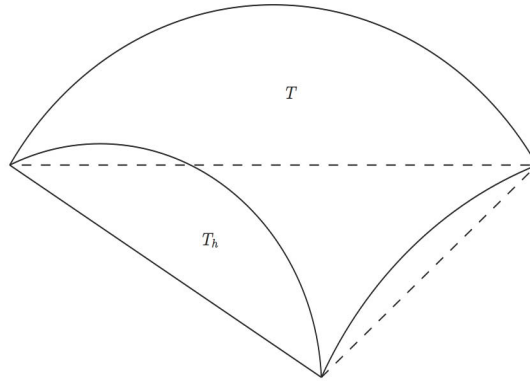


Fig. 1: A surface triangle T , and a planar triangle T_h .

3. Error Analysis

Let $\mathcal{T} = \{T_1, T_2, \dots, T_n\}$ and $\mathcal{T}_h = \{T_{h_1}, T_{h_2}, \dots, T_{h_n}\}$ denote the triangulation of the surfaces S and S_h respectively. That is,

$$S = \cup_{i=1}^n T_i \quad \text{and} \quad S_h = \cup_{i=1}^n T_{hi}.$$

Also, let T and T_h denote the triangles on the surfaces S , and S_h , respectively such that $T = P(T_h)$. Thus, T is the projection of T_h onto S . Surface triangle T , and the planar triangle T_h share the same vertices. Figure shows the planar triangle T_h and the triangle T . If $\{\eta_i\}_{i=1}^m$ are the nodes of the triangulation \mathcal{T} covering the surface, S , then $S_h \cap S = \{\eta_i\}_{i=1}^m$.

Let $\delta > 0$ be sufficiently small to ensure that the decomposition

$$x = P(x) + d(x)n$$

is uniquely determined. Let \hat{u} be a smooth extension of u by

$$\hat{u}(x) = u(P(x)) \quad \text{for every } x \in U. \tag{14}$$

Clearly $\hat{u}(y) = u(y)$ for every $y \in S$ and note that \hat{u} is constant along the normal direction to the surface S , that is $\nabla \hat{u} \cdot n = 0$, where n is the unit outward normal vector to the surface S at the point $P(x)$.

The tangential gradient of the function u is the orthogonal projection of the gradient of u onto the tangent plane.

With $n = (n_1, \dots, n_{N+1})$, the tangential gradient, $\nabla_S u = \nabla \hat{u} - (\nabla \hat{u} \cdot n)n$, can be expressed as:

$$\nabla_S u = A \nabla \hat{u}, \tag{15}$$

where A is the $(N + 1) \times (N + 1)$ matrix with $(A)_{ij} = \begin{cases} 1 - n_i^2 & i = j \\ -n_i n_j & i \neq j \end{cases}$.

The following lemma is proved in (Dziuk, 1988) (Lemma 1):

Lemma 0.1: Let u and \hat{u} be functions such that $\hat{u} = u(P(x))$ for $x \in U$, and let $T = P(x)$, then there exists some constants $0 < c_i, i = 1 \dots, 5$ such that

$$\begin{aligned} c_1 \|\hat{u}\|_{L^2(T_h)} &\leq \|u\|_{L^2(T)} \leq c_2 \|\hat{u}\|_{L^2(T_h)}, \\ c_3 \|\hat{u}\|_{H^1(T_h)} &\leq \|u\|_{H^1(T)} \leq c_4 \|\hat{u}\|_{H^1(T_h)}, \end{aligned}$$

(implying the equivalence of norms) and

$$\|\hat{u}\|_{H^2(T_h)} \leq c_5 \|u\|_{H^2(T)}.$$

We define the piecewise interpolant $Iu \in \chi_h$ of a function $u \in C(S)$ by;

$$Iu(\eta_i) = u(\eta_i) \quad i = 1, 2, \dots, n,$$

where $\{\eta_i\}_{i=1}^n$ are the nodes of the surface triangulation \mathcal{T} .

Proposition 0.1: For any continuous function u defined on a surface triangle T in which $T = P(T_h)$ and the smooth extension \hat{u} of u we have;

$$\hat{u}|_{T_h} = u \circ P|_{T_h}.$$

We then denote the restriction of interpolation to the planar triangle T_h as I_{T_h} and is given by

$$I_{T_h} \hat{u} = (Iu \circ P)|_{T_h},$$

where I_{T_h} is the piecewise linear interpolation of continuous functions defined on the planar triangle T_h .

Proof: Let $\{\varphi_i\}_{i=1}^3$ be the projected surface finite element basis functions of the surface triangle T . Let $\{\eta_i\}_{i=1}^3$ be the vertices of the surface triangle T and T_h , since T and planar triangle T_h share the same vertices (see Figure). Let $\{\varphi_{h_i}\}_{i=1}^3$ be the linear finite element basis functions for the planar triangle T_h , and by definition we have

$$\varphi_i = \varphi_{h_i} \circ P^{-1}, \quad i = 1, 2, 3.$$

Let $u \in C(S)$, then $Iu = \sum_{i=1}^3 u(\eta_i) \varphi_i$, composing both sides with P we get,

$$\begin{aligned} Iu \circ P &= \sum_{i=1}^3 u(\eta_i) \varphi_i \circ P \quad \text{since } \varphi_i = \varphi_{h_i} \circ P^{-1} \\ &= \sum_{i=1}^3 \hat{u}(\eta_i) \varphi_{h_i} \\ &= I_{T_h} \hat{u}. \end{aligned}$$

We set $I_{T_h} \hat{u} = (Iu \circ P)|_{T_h}$. □

The following estimate is a well known consequence of the Bramble-Hilbert Lemma (see (Braess, 2001; Brenner and Scott, 1994; Ciarlet, 2002) for details)

$$\|I_{T_h}\hat{u} - \hat{u}\|_{L^2(T_h)} \leq ch^2\|\hat{u}\|_{H^2(T_h)}. \quad (16)$$

Theorem 0.1: Let $u \in H(S)$ and let $Iu \in \chi_h$ be the interpolant of u , then

$$\|Iu - u\|_{L^2(S)} \leq ch^2\|u\|_{H^2(S)} \quad (17)$$

and

$$\|\nabla_S(Iu - u)\|_{L^2(S)} \leq ch\|u\|_{H^2(S)}. \quad (18)$$

Proof: We only prove inequality (17), since the proof of inequality (18) is similar. For any u defined on the surface triangle T , we have that $\hat{u}|_{T_h} = u \circ P|_{T_h}$

$$\begin{aligned} \|Iu - u\|_{L^2(S)}^2 &\leq c \sum_T \|Iu - u\|_{L^2(T)}^2 \quad \text{by Lemma 0.1} \\ &\leq c \sum_{T_h} \|Iu \circ P - u \circ P\|_{L^2(T_h)}^2 \quad \text{since } \hat{u}|_{T_h} = u \circ P|_{T_h} \\ &\leq c \sum_{T_h} \|I_{T_h}\hat{u} - \hat{u}\|_{L^2(T_h)}^2 \quad \text{and by (16)} \\ &\leq ch^4 \sum_{T_h} \|\hat{u}\|_{H^2(T_h)}^2 \quad \text{by Lemma 0.1} \\ &\leq ch^4 \sum_T \|u\|_{H^2(T)}^2. \end{aligned}$$

Hence, $\|Iu - u\|_{L^2(S)} \leq ch^2\|u\|_{H^2(S)}$. □

Remark 0.1: Clearly, the interpolant Iu is well defined for continuous functions, since it uses the nodal values of the function u . Since $u \in H^2(S)$, u is continuous on S by Sobolev embedding theorem (Hebey, 1991). Note also that $u \circ P|_{T_h}$ is in $H^2(T_h)$ whenever $u \in H^2(S)$ (by Lemma 0.1) and thus $u \circ P|_{T_h}$ is also continuous on T_h .

We are now ready to prove the convergence rates:

Theorem 0.2: Assume the solution of (10) is $u \in H^2(S)$, and let \tilde{u} be the solution of (12) (for a shape regular triangulation of the planar surface S_h), then

$$\|u - \tilde{u}\|_{L^2(S)} \leq ch^2\|u\|_{H^2(S)}$$

and

$$\|u - \tilde{u}\|_{H^1(S)} \leq ch\|u\|_{H^2(S)}.$$

Proof: Using Cea's Lemma, the fact that for any function u defined on T we have that $\hat{u}|_{T_h} = u \circ P|_{T_h}$ we obtain that

$$\begin{aligned} \|u - \tilde{u}\|_{H^1(S)} &\leq c \inf_{v \in \chi_h} \|u - v\|_{H^1(S)} \\ &\leq c \inf_{v \in \chi_h} \sum_T \|u - v\|_{H^1(T)} \\ &\leq c \sum_{T_h} \|Iu - u\|_{H^1(T_h)} \quad \text{by (18)} \\ &\leq ch \sum_T \|u\|_{H^2(T)} \\ &\leq ch \|u\|_{H^2(S)}. \end{aligned}$$

Using a duality argument, see (Brenner and Scott, 1994), we get

$$\begin{aligned} \|u - \tilde{u}\|_{L^2(S)} &\leq ch \|u - \tilde{u}\|_{H^1(S)} \\ &\leq ch^2 \|u\|_{H^2(S)}. \end{aligned}$$

□

4. Eigenvalue Problem

We consider the following eigenvalue problem

$$-\Delta_S u = \lambda u, \quad (19)$$

where $-\Delta_S$ is the Laplace-Beltrami operator on the unit sphere S . The Laplace-Beltrami operator is a positive self adjoint operator, it has a sequence of nonnegative real eigenvalues $\{\lambda\}_{k=0}^{\infty}$. The (exact) eigenvalues are $\lambda_k = k(k+1)$, $k = 0, 1, \dots, \infty$, and the k^{th} eigenvalue λ_k has algebraic multiplicity $2k+1$. The corresponding eigenfunctions are the spherical harmonics $S_{n,m}$ of degree n and order m , where $|m| \leq n$ (see (Pinchover and Rubinstein, 2005)).

The weak formulation of (19) is, find $\lambda \in \mathbb{R}$, and $u \in H^1(S)$, $u \neq 0$ such that

$$a(u, v) = \lambda(u, v) \quad \forall v \in H^1(S). \quad (20)$$

Here $a(\cdot, \cdot) : H^1(S) \times H^1(S) \rightarrow \mathbb{R}$ is a bilinear, continuous, elliptic form given by

$$a(u, v) = \int_S \nabla_S u \cdot \nabla_S v.$$

Problem (20) has a sequence of eigenvalues (counting multiplicity) which we denote

$$\lambda_0 \leq \lambda_{1,1} = \lambda_{1,2} = \lambda_{1,3} \leq \dots \leq \lambda_{k,1} = \dots = \lambda_{k,2k+1} \leq \dots,$$

and we denote the corresponding eigenfunctions, which are spherical harmonics, by

$$u_0, u_1, \dots$$

These eigenfunctions are orthogonal in the energy inner product

$$a(u_i, u_j) = \lambda_i(u_i, u_j) = \lambda_i \delta_{ij}.$$

We are interested in approximating the eigenvalues and eigenfunctions of (20) using the finite element method. Let χ_h be finite dimensional subspace $\chi_h \subset H^1(S)$ as defined in Section . Consider the following discrete eigenvalue problem, find $\tilde{\lambda} \in \mathbb{R}$ and $\tilde{u} \in \chi_h$, $\tilde{u} \neq 0$ such that

$$a_h(\tilde{u}, \tilde{v}) = \lambda_h(\tilde{u}, \tilde{v}) \quad \forall \tilde{v} \in \chi_h, \quad (21)$$

where $a_h(\tilde{u}, \tilde{v}) = \int_S \nabla_S \tilde{u} \cdot \nabla_S \tilde{v}$. Problem (21) has a sequence of eigenvalues,

$$\tilde{\lambda}_0 \leq \tilde{\lambda}_1 \leq \dots \leq \tilde{\lambda}_n \quad n = \dim \chi_h$$

and corresponding eigenvectors,

$$\tilde{u}_0, \tilde{u}_1, \dots, \tilde{u}_n,$$

which are also orthogonal in the energy inner product,

$$a_h(\tilde{u}_i, \tilde{u}_j) = \lambda_i(\tilde{u}_i, \tilde{u}_j) = \lambda_i \delta_{ij} \quad i, j = 1, \dots, n.$$

The eigenpairs $(\tilde{\lambda}, \tilde{u})$ of (21) are the approximations to the eigenpairs (λ, u) of (20). The eigenvalues λ_k and their approximates $\tilde{\lambda}_k$ satisfy the following well-known minmax principles:

$$\lambda_k = \min_{U_k \subset H^1(S)} \max_{u \in U_k} \frac{a(u, u)}{(u, u)} \quad \text{and} \quad \tilde{\lambda}_k = \min_{S_k \subset \chi_h} \max_{\tilde{u} \in S_k} \frac{a(\tilde{u}, \tilde{u})}{(\tilde{u}, \tilde{u})}.$$

The minimum is taken over all k -dimensional subspaces U_k , and S_k , of $H^1(S)$, and χ_h respectively. It follows immediately from the minmax principles that *every eigenvalue is approximated from above* by $2k + 1$ of the approximate eigenvalues, see (Strang and Fix, 1973). Hence

$$\lambda_k \leq \tilde{\lambda}_{k,1} \leq \tilde{\lambda}_{k,2} \leq \dots \leq \tilde{\lambda}_{k,2k+1} \quad \lambda_k \simeq \tilde{\lambda}_{k,1}, \tilde{\lambda}_{k,2}, \dots, \tilde{\lambda}_{k,2k+1}.$$

It is also well known that,

$$\tilde{\lambda}_{k,q} - \lambda_k \leq C \sup_{u \in M(\lambda_k)} \inf_{v_h \in \chi_h} \|u - v_h\|_a^2 \quad q = 1 \dots 2k + 1,$$

where $\|\cdot\|_a$ denotes the energy norm and $M(\lambda_k)$ is the space of eigenfunctions corresponding to eigenvalue λ_k (Babuska and Osborn, 1987), (Babuska and Osborn, 1989).

5. Numerical Experiments

5.1. Example 1

To illustrate our method, we present numerical experiments for the following model problem

$$-\Delta_S u + u = f \quad \text{on } S. \quad (22)$$

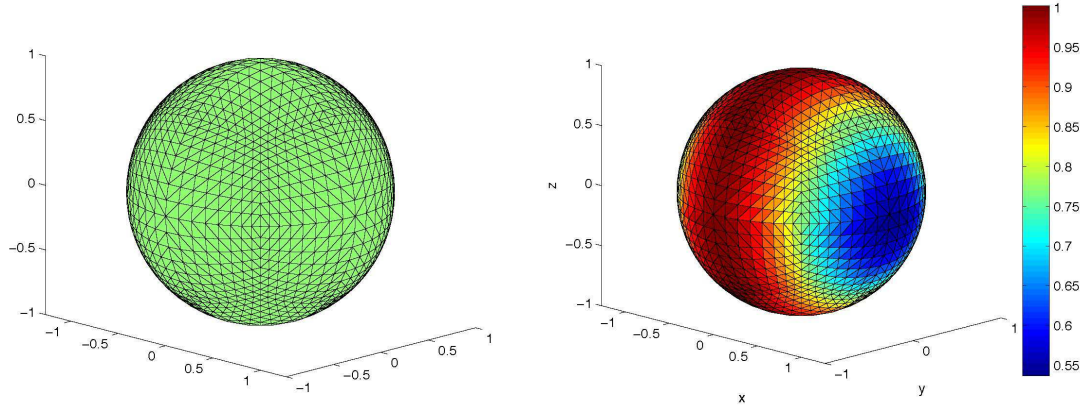


Fig. 2: Shape regular mesh on the sphere and approximate solution \tilde{u} at refinement step $j = 4$.

where S is the unit sphere in \mathbb{R}^3 , and $d(x) = \sqrt{x^2 + y^2 + z^2} - 1$ is the signed distance function for the unit sphere. We choose a right hand side f such that the exact solution of the above problem is $u(x, y, z) = \cos x$. Let's remark that the right hand side function f is derived by;

$$f = -\nabla_S \cdot v + u \text{ where } v = \nabla_S u \text{ and } \nabla_S \cdot v = \nabla \cdot v - \sum_{i=1}^3 (\nabla v_i \cdot n) n_i.$$

We denote by \tilde{u} the approximate solution, and by h^j the largest diameter of the spherical triangles at the j^{th} refinement step which is measured by the following geodesic distance formula;

$$g(x, y) = \arccos(x \cdot y), \tag{23}$$

where x and y are two points on S . The discrete weak formulation of (22) is: Find $\tilde{u} \in \chi_h$ s.t.

$$\int_S \nabla_S \tilde{u} \nabla_S v + \tilde{u} v ds = \int_S f v ds, \quad \text{for all } v \in \chi_h \tag{24}$$

where χ_h is the finite dimensional subspace of $H^1(S)$, as defined in (13), thus

$$\chi_h = \{ \tilde{u} : \tilde{u} = u_h \circ P^{-1}, u_h \text{ is a piecewise linear, continuous polynomial in } S_h \}.$$

Let $\tilde{u} = \sum_{i=1}^n \tilde{u}_i \varphi_i$ then (24) becomes the following linear system of algebraic equation

$$\mathbf{M}\mathbf{x} = \mathbf{f},$$

where $\mathbf{M} = \mathbf{A} + \mathbf{B}$ with components

$$A_{ij} = \int_S \nabla_S \varphi_j \cdot \nabla_S \varphi_i ds$$

$$B_{ij} = \int_S \varphi_j \cdot \varphi_i ds.$$

The components of right hand side vector \mathbf{f} is

$$f_i = \int_S f \varphi_i ds,$$

TABLE I: Observed convergence rates for Example 1, j denotes the refinement step, h^j denotes the largest diameter of the spherical triangles, n denotes the number of spherical triangles, p denotes the experimental convergence rate in the L^2 -norm, and q denotes the experimental convergence rate in the H^1 -norm .

j	n	h	$\ u - u_h\ _{L^2(S)}$	p	$\ u - u_h\ _{H^1(S)}$	q
1	48	0.9553	0.082200	-	0.4872	-
2	192	0.6155	0.027100	2.5242	0.2933	1.1544
3	768	0.3398	0.007500	2.1624	0.1523	1.1031
4	3072	0.1750	0.002000	1.9919	0.0775	1.0181
5	12288	0.0882	0.000499	2.0260	0.0390	1.0022.
6	49152	0.0441	0.000125	2.0001	0.0196	0.9959
7	196,608	0.0221	0.000031	1.9987	0.0098	1.0000

where ds is the surface measure on S . Note that in our approach, the linear approximation S_h of the surface S is used as a tool and all calculations are done on S_h .

$$\begin{aligned}
 A_{ij} &= \int_S \nabla_S \varphi_j \cdot \nabla_S \varphi_i ds \\
 &= \sum_T \int_T (\nabla \varphi_j - (\nabla \varphi_j \cdot n)n) \cdot (\nabla \varphi_i - (\nabla \varphi_i \cdot n)n) ds \\
 &= \sum_{T_h} \int_{T_h} (J^{-1} \nabla \varphi_{hj} - (J^{-1} \nabla \varphi_{hj} \cdot n)n) \cdot (J^{-1} \nabla \varphi_{hi} - (J^{-1} \nabla \varphi_{hi} \cdot n)n) |J| ds_h,
 \end{aligned}$$

Note that the projection from the planar triangle T_h onto surface triangle T is:

$$P(x, y, z) = \left(\frac{x}{\sqrt{x^2 + y^2 + z^2}}, \frac{y}{\sqrt{x^2 + y^2 + z^2}}, \frac{z}{\sqrt{x^2 + y^2 + z^2}} \right).$$

The inverse projection from the surface triangle T onto planar triangle T_h is

$$P^{-1}(x, y, z) = \left(\frac{-dx}{ax + by + cz}, \frac{-dy}{ax + by + cz}, \frac{-dz}{ax + by + cz} \right),$$

where $ax + by + cz + d = 0$ is the equation of the plane that the surface triangle T is projected into.

The transpose of the Jacobian of the inverse projection P^{-1} is denoted by J^{-1} , and J is the

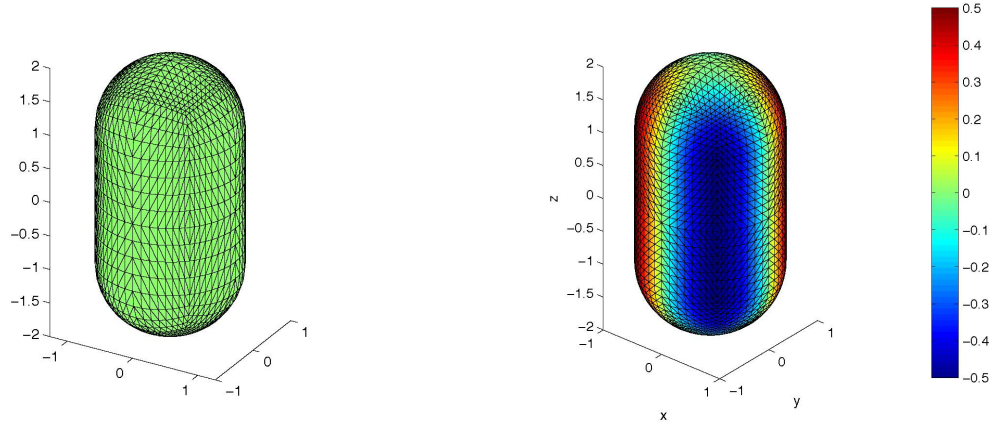


Fig. 3: Shape regular mesh generated on surface, S in Example 2 and the approximate solution at refinement step $j = 4$.

determinant of the Jacobian matrix of the projection P . Similarly,

$$\begin{aligned}
 B_{ij} &= \int_S \varphi_j \cdot \varphi_i ds \\
 &= \sum_T \int_T \varphi_j \cdot \varphi_i ds \\
 &= \sum_{T_h} \int_{T_h} \varphi_{hj} \cdot \varphi_{hi} |J| ds_h \\
 &= \int_{S_h} \varphi_{hj} \cdot \varphi_{hi} |J| ds_h,
 \end{aligned}$$

and

$$\begin{aligned}
 f_i &= \int_S f \varphi_i ds \\
 &= \sum_T \int_T f \varphi_i ds \\
 &= \sum_{T_h} \int_{T_h} f \varphi_{hi} |J| ds_h \\
 &= \int_{S_h} f \varphi_{hi} |J| ds_h.
 \end{aligned}$$

Here ds_h is the surface measure for S_h , and $\{\varphi_{hi}\}_{i=1}^n$ are the the basis for χ_h . The mesh used is a shape regular mesh (see Fig 2 for the resulting mesh on the sphere). These integrals are computed using Gauss quadrature and the linear system is solved using a direct solver in Matlab.

The experimentally observed convergence rates in the L^2 -norm, and H^1 - norm , p and q are

$$p = \frac{\ln\left(\frac{e_2^j}{e_2^{j+1}}\right)}{\ln\left(\frac{h^j}{h^{j+1}}\right)} \quad \text{and} \quad q = \frac{\ln\left(\frac{e_1^j}{e_1^{j+1}}\right)}{\ln\left(\frac{h^j}{h^{j+1}}\right)}, \quad (25)$$

TABLE II: Observed convergence rates for Example 2, j denotes the refinement step, h^j denotes the mesh size, n denotes the number of surface triangles, p denotes the experimental convergence rate in the L^2 -norm, and q denotes the experimental convergence rate in the H^1 -norm.

j	n	h	$\ u - u_h\ _{L^2(S)}$	p	$\ u - u_h\ _{H^1(S)}$	q
1	80	1.2593	0.3452	-	1.5668	-
2	320	0.6791	0.0917	2.1466	0.7657	1.1594
3	1280	0.3496	0.0238	2.0314	0.3886	1.0215
4	5120	0.1763	0.0060	2.0127	0.1954	1.0042
5	20480	0.0883	0.0015	2.0049	0.0979	0.9995
6	81920	0.0442	3.7979-4	1.9851	0.0490	1.0002
7	327680	0.0221	9.4983-5	1.9993	0.0245	1.0000

TABLE III: Observed errors and convergence rates for Example 3. Here j denotes the refinement step, h^j denotes the diameter of the largest triangle measured using the geodesic distance formula (23), n denotes the number of spherical triangles e_{min} and e_{max} denote the error, and p_{min} and p_{max} denote the convergence rate computed using (25) using e_{min} and e_{max} respectively.

j	n	h^j	2		6		12		20	
			e_{min}/e_{max}	p_{min}/p_{max}	e_{min}/e_{max}	p_{min}/p_{max}	e_{min}/e_{max}	p_{min}/p_{max}	e_{min}/e_{max}	p_{min}/p_{max}
1	48	0.9553	0.065307/0.065307	-	0.917904/1.627359	-	2.65811/9.90629	-	5.65335/33.47223	-
2	192	0.6155	0.018207/0.018207	2.91/2.91	0.267567/0.438625	2.80/2.98	1.20605/2.29539	1.80/3.33	3.41964/5.85049	1.14/3.97
3	768	0.3398	0.00501/0.00501	2.17/2.17	0.072137/0.113837	2.21/2.27	0.32043/0.55944	2.23/2.38	1.01191/1.43773	2.05/2.37
4	3072	0.1750	0.001312/0.001312	2.02/2.02	0.018873/0.028854	2.02/2.07	0.08306/0.13996	2.03/2.09	0.26713/0.36505	2.01/2.07
5	12288	0.0882	0.000333/0.000333	2.00/2.00	0.004803/0.007245	1.99/2.02	0.02108/0.03504	2.00/2.02	0.06843/0.09168	1.99/2.02
6	49152	0.0442	0.000084/0.000084	1.99/1.99	0.001208/0.001813	1.99/2.01	0.0053/0.00877	1.99/2.00	0.01725/0.02295	1.99/2.00
7	1966608	0.0221	0.000021/0.000021	2.00/2.00	0.000303/0.000454	1.99/1.99	0.00133/0.00219	1.99/2.00	0.00432/0.00574	1.99/1.99

where e_2^j , and e_1^j denotes the error measured in the L^2 -norm, and H^1 - norm, respectively, at j^{th} refinement step. We present the results in Table I.

5.2. Example 2

For the second experiment we use an arbitrary surface S given by

$$S = \begin{cases} x^2 + y^2 + (z - 1)^2 = 1 & \text{if } 1 < z \leq 2 \\ x^2 + y^2 = 1 & \text{if } -1 \leq z \leq 1 \\ x^2 + y^2 + (z + 1)^2 = 1 & \text{if } -1 < z \leq -2 \end{cases}$$

A shape regular mesh generated for the surface S is shown in Figure 3. We solve the following P.D.E

$$-\Delta_S u + u = f \quad \text{on } S, \tag{26}$$

for given $f = \begin{cases} 7xy & \text{if } 1 < z \leq 2 \text{ and } -2 \leq z < -1 \\ 5xy & \text{if } -1 \leq z \leq 1 \end{cases}$

TABLE IV: The exact eigenvalues 2, 6, 12, and 20 and their approximates. Here j denotes the refinement step, h^j denotes the diameter of the largest spherical triangle measured using the geodesic distance formula (23), n denotes the number of spherical triangles.

j	n	h^j	2	6	12	20
1	48	0.9553	2.065307	6.917904	14.65811	25.65335
			2.065307	6.917904	16.31414	28.57216
			2.065307	7.627359	16.31414	28.57216
				7.627359	16.31414	37.4226
				7.627359	21.90629	37.4226
					21.90629	37.4226
					21.90629	53.47223
2	192	0.6155	2.018207	6.267567	13.20605	23.41964
			2.018207	6.267567	13.20605	23.8761
			2.018207	6.438625	13.20605	23.8761
				6.438625	13.54976	25.46191
				6.438625	14.29539	25.46191
					14.29539	25.46191
					14.29539	25.85049
3	768	0.3398	2.00501	6.072137	12.32043	21.01191
			2.00501	6.072137	12.32043	21.1005
			2.00501	6.113837	12.32043	21.1005
				6.113837	12.45896	21.35449
				6.113837	12.55944	21.35449
					12.55944	21.35449
					12.55944	21.43773
4	3072	0.1750	2.001312	6.018873	12.08306	20.26713
			2.001312	6.018873	12.08306	20.28555
			2.001312	6.028854	12.08306	20.28555
				6.028854	12.11908	20.33697
				6.028854	12.13996	20.33697
					12.13996	20.33697
					12.13996	20.36505
5	12288	0.0882	2.000333	6.004803	12.02108	20.06843
			2.000333	6.004803	12.02108	20.07245
			2.000333	6.007245	12.02108	20.07245
				6.007245	12.03005	20.08426
				6.007245	12.03504	20.08426
					12.03504	20.08426
					12.03504	20.09168
6	49152	0.0441	2.000084	6.001208	12.0053	20.01725
			2.000084	6.001208	12.0053	20.0182
			2.000084	6.001813	12.0053	20.0182
				6.001813	12.00753	20.02107
				6.001813	12.00877	20.02107
					12.00877	20.02107
					12.00877	20.02295
7	196608	0.0221	2.000021	6.000303	12.00133	20.00432
			2.000021	6.000303	12.00133	20.00456
			2.000021	6.000454	12.00133	20.00456
				6.000454	12.00188	20.00527
				6.000454	12.00219	20.00527
					12.00219	20.00527
					12.00219	20.00574

With this choice of right hand side function. f , the exact solution is $u = xy$. We approximate the solution of (26) by using the finite element method described in Section 2. Since, S is a piecewise defined surface, the projections are as well piecewise defined. For $-1 \leq z \leq 1$, projection from S_h to S and its inverse are given by,

$$P(x, y, z) = \left(\frac{x}{\sqrt{x^2 + y^2}}, \frac{y}{\sqrt{x^2 + y^2}}, z \right),$$

$$P^{-1}(x, y, z) = \left(\frac{-x(cz + d)}{ax + by}, \frac{-y(cz + d)}{ax + by}, z \right),$$

where $ax + by + cz + d = 0$ is the equation of the plane where the planar triangle lies onto. For $1 \leq z \leq 2$, projection from S_h to S and its inverse are given by

$$P(x, y, z) = \left(\frac{x}{\sqrt{x^2 + y^2 + z^2}}, \frac{y}{\sqrt{x^2 + y^2 + z^2}}, \frac{z}{x^2 + y^2 + z^2} \right),$$

$$P^{-1}(x, y, z) = \left(\frac{-x(c + d)}{ax + by + c(z - 1)}, \frac{-y(c + d)}{ax + by + c(z - 1)}, \frac{ax + by - zd + d}{ax + by + c(z - 1)} \right).$$

Similar transformations when $-2 \leq z \leq -1$. We estimate the convergence using the formula (25), and present the results in Table II.

5.3. Example 3

For the third example, we approximate the eigenvalues of the following problem by using the finite element method described in this paper.

$$-\Delta_S u = \lambda u, \quad (27)$$

where S is the unit sphere. With $\tilde{u} = \sum_{i=1}^n \tilde{u}_i \varphi_i$ and $\tilde{v} = \varphi_i$, the discrete eigenvalue problem, (21), becomes the following generalized eigenvalue problem

$$A\mathbf{x} = \lambda^h B\mathbf{x},$$

where $A_{ij} = \int_S \nabla_S \varphi_j \cdot \nabla_S \varphi_i$, $B_{ij} = \int_S \varphi_j \varphi_i$, and $x_i = \tilde{u}_i$. The eigenvalues of this generalized, algebraic eigenproblem were approximated in Matlab. Recall the exact eigenvalues of (27) are $\lambda_k = k(k + 1)$ for $k = 0, 1, 2, \dots$, with multiplicity $2k + 1$. The approximates of the first 5 eigenvalues (which are 0, 2, 6, 12, and 20) which were obtained with the finite element method described in this paper are presented in Table IV.

The observed errors and convergence rates for the approximate eigenvalues are presented in Table III, where e_{min} is the error between the exact eigenvalue and its smallest approximate value and e_{max} is the error between the exact eigenvalue and its largest approximate value. Similarly, p_{min} and p_{max} are the observed convergence rates using e_{min} and e_{max} , respectively.

6. Conclusion

Developing new algorithms to approximate solutions of partial differential equations defined on surfaces is a challenging problem. In this paper, we propose and analyze the projected surface finite element method to solve such problems. We obtain the convergence rates for the projected surface finite elements and show that the approximate solutions converge accurately to the exact solution as the mesh size is refined. We also compute the convergence rates in the experiments and show that it approaches, asymptotically, the proven values.

Projected surface finite elements depend on the transformations projecting planar triangle to the surface triangle and its inverse. These transformations vary for each surface. In this paper, we demonstrate explicitly what these transformations are for a sphere and a cylinder with spherical caps.

The method developed in this paper can also be applied to the eigenvalue problem defined on surfaces. Since the eigenvalues of the Laplace-Beltrami operator on the unit sphere is well known, we illustrate that the projected surface finite elements approximates the eigenvalues of the Laplace-Beltrami on the unit sphere well.

REFERENCES

- Apel, T. and Pester, C. (2005). Clement-type interpolation on spherical domains-interpolation error estimates and application to a posteriori error estimation. *IMA J. Numer. Anal.*, 25:310–336.
- Aubin, T. (1980). *Nonlinear analysis on manifolds, Monge-Ampère Equations*. Springer-Verlag.
- Babuska, I. and Osborn, J. E. (1987). Estimates for the errors in eigenvalue and eigenvector approximation by galerkin methods, with particular attention to the case of multiple eigenvalues. *SIAM Journal on Numerical Analysis*, 24:1249–1276.
- Babuska, I. and Osborn, J. E. (1989). Finite element-galerkin approximation of the eigenvalues and eigenvectors of selfadjoint problems. *Mathematics of Computation*, 52:275–297.
- Braess, D. (2001). *Finite Elements. Theory, fast solvers, and applications in solid mechanics*. Cambridge.
- Brenner, S. and Scott, L. R. (1994). *The mathematical theory of finite element methods*. Springer, Verlag.
- Ciarlet, P. (2002). *The Finite Element Method for Elliptic Problems*. SIAM.
- Demlow, A. (2009). Higher-order finite element methods and pointwise error estimates for elliptic problems on surfaces. *SIAM J. Numer. Anal.*, 47(2):805–827.
- Demlow, A. and Dziuk, G. (2007). An adaptive finite element method for the Laplace-Beltrami operator on implicitly defined surfaces. *SIAM J. Numer. Anal.*, 45(1):421–442 (electronic).
- Du, Q. and Ju, L. (2005). Finite volume methods on spheres and spherical centroidal voronoi meshes. *SIAM Journal on Numerical Analysis*, 43:1673–1692.
- Dziuk, G. (1988). Finite elements for the beltrami operator on arbitrary surfaces. *Partial differential equations and calculus of variations, Lecture notes in Mathematics*, 1357:142–155.

- Dziuk, G. and Elliott, C. M. (2007). Finite elements on evolving surfaces. *Journal of Numerical Analysis*, 27:262–292.
- Gilbarg, D. and Trudinger, N. S. (1977). *Elliptic Partial differential Equation of second order*. Springer.
- Hebey, E. (1991). *Sobolev Spaces on Riemannian Manifolds*. Springer.
- Holst, M. (2001). Adaptive numerical treatment of elliptic systems on manifolds. *Advances in Computational Mathematics*, 15:139–191.
- Meir, A. and Tuncer, N. (2009). Radially projected finite elements. *SIAM Journal of Scientific Computing*, 31:2368–2385.
- Pinchover, Y. and Rubinstein, J. (2005). *An introduction to Partial differential equations*. Cambridge.
- Strang, G. and Fix, G. (1973). *An analysis of the Finite Element Method*. Prentice Hall.